Published in final edited form as:

J Leukoc Biol. 2020 April ; 107(4): 551–560. doi:10.1002/JLB.3HI1119-389RRRR.

Proliferation of Ly6C+ monocytes/macrophages contributes to their accumulation in mouse skin wounds

Jingbo Pang[*], **Norifumi Urao**[*], **Timothy J. Koh**[*,¶]

[*]Center for Wound Healing and Tissue Regeneration, Department of Kinesiology and Nutrition, University of Illinois at Chicago, Chicago, IL 60612;

Abstract

Monocytes and macrophages (Mo/MΦ) play critical roles in all phases of skin wound healing. The majority of these cells are thought to be recruited from blood Mo; however, the role local proliferation of Mo/MΦ in the wound has not been defined. Therefore, we tested the hypothesis that local proliferation of Mo and/or MΦ contributes to their accumulation during wound healing. Male C57Bl/6 mice (N=4–9/group) were subjected to excisional skin wounding. Proliferating Mo/MΦ (F4/80+Ki67+) were observed in wound cryosections, peaking on day 5 post-wounding. Cell cycle analysis on cells isolated from skin tissue revealed that wounding increased both the number and percentage of inflammatory Ly6C+F4/80lo/- Mo/MΦ in the S/G2/M phases, peaking on day 6 post-wounding. In contrast, more mature Ly6C-F4/80+ cells were found predominantly in the G0 phase with less than 1% cells in S/G2/M phase following injury. In peripheral blood, Mo were very rarely found in the S/G2/M phase, suggesting that the wound environment triggered the Ly6C+F4/80lo/- Mo proliferative response. Furthermore, injury induced several potential regulators of proliferation in wounds, including IL-1β and IL-6, and wound Mo/MΦ expressed surface receptors for these cytokines. However, wound Mo/MΦ proliferation was not altered in IL-1R1 KO or IL-6 KO mice. In summary, our findings indicate that proliferation contributes to Mo/MΦ accumulation in wounds and, contrary to findings in other pathophysiological conditions, Ly6C+/F4/80lo/- Mo/MΦ proliferate during skin wound healing whereas mature Ly6C-F4/80+ MΦ do not.

Graphical Abstract

[¶]Address correspondence and reprint requests to Dr. Timothy J. Koh, University of Illinois at Chicago, Center for Wound Healing and Tissue Regeneration, Department of Kinesiology and Nutrition, 1919 W. Taylor Street, Chicago, IL 60612-7246; Phone number: 312-413-9771; Fax: 312-413-3699; tjkoh@uic.edu.

Authorship

JP designed the study, conducted the experiments, performed data and statistical analysis and wrote the manuscript. NU contributed to study design and manuscript review. TK helped design the study, edit and revise the manuscript, and provided all materials.

Disclosure

All authors have no financial conflicts of interest to report.

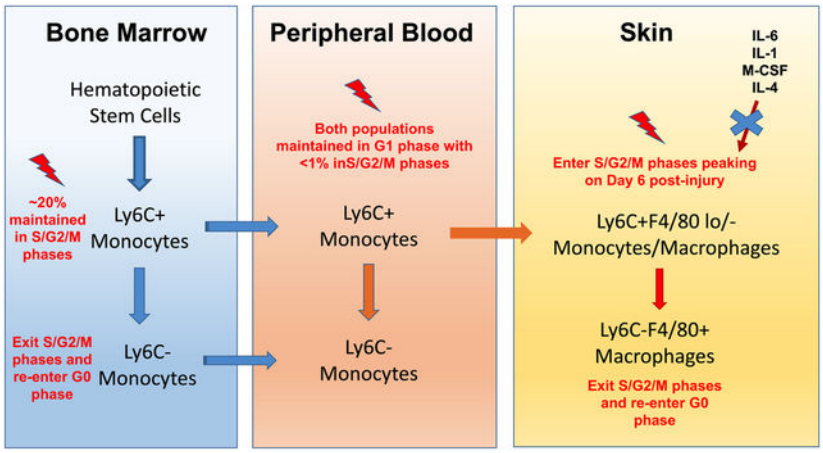

Summary

Inflammatory monocytes/macrophages proliferate while mature macrophages do not in mouse skin wounds.

Keywords

Inflammation; Cell Cycle; IL-1; IL-6

Introduction

Skin wound healing is an evolutionarily conserved and tightly coordinated process composed of overlapping stages of inflammation, proliferation, and remodeling (1). Following injury, a variety of cells, including inflammatory cells, fibroblasts, endothelial cells, and keratinocytes, work together to heal the wound (1, 2). Among these cells, monocytes and macrophages (Mo/MΦ) rapidly accumulate in wounds and play critical roles in the repair process (3, 4). During the inflammatory phase of healing, Mo/MΦ kill pathogens, amplify the inflammatory response and help to clear debris and dead cells. During the proliferation phase, Mo/MΦ help to downregulate inflammation, promote angiogenesis, formation of granulation tissue and deposition of collagen. Later, Mo/MΦ also promote wound closure and collagen remodeling (2, 5, 6). In short, Mo/MΦ play a vital role in all stages of healing.

The majority of Mo/MΦ that accumulate in skin wounds are thought to derive from circulating blood Mo in mice (2, 7, 8). Mo are produced in bone marrow by sequential differentiation from hematopoietic stem cells, under the control of a variety of growth factors and transcription factors (9). Such differentiation produces Ly6Chi Mo that can eventually differentiate to Ly6Clo Mo in different tissues (10, 11). Ly6Chi Mo are mobilized into peripheral blood both during homeostasis and during inflammatory responses via CCL2/CCR2 signaling (9, 12). Following tissue injury, large numbers of blood-borne Ly6Chi Mo are recruited to the damaged tissue in response to a variety of damage and pathogen-associated molecular patterns (DAMPs/PAMPs), chemokines and cytokines (including CCL2) (7, 12). Tissue damage also results in increased bone marrow

monopoiesis, which helps to supply Mo for tissue repair and to repopulate bone marrow and blood stores (13). Although most Mo/MΦ in skin wounds are thought to be derived from bone marrow Mo, a small population of skin resident MΦ also likely act as first responders upon wounding, contributing to the initiation of inflammation (8).

In addition to the recruitment of blood Mo, cell proliferation may contribute to tissue Mo/MΦ accumulation under certain conditions (14–18). For example, Jenkins et al. have demonstrated that both pleural resident MΦ and MΦ recruited to the peritoneal cavity can proliferate during TH2 related pathologies such as *L. sigmodontis* and *Brugia malayi* infection (17). Additional studies have indicated that resident MΦ can proliferate in lung, aorta, adipose tissue, and brain under inflammatory conditions (14–17, 19–21). In these studies, the microenvironment appears to be a major driver of proliferation (14–17, 20, 22). However, whether proliferation contributes to MΦ accumulation during skin wound healing remains to be determined.

The purpose of this study was to determine whether Mo/MΦ proliferate during wound healing, thus contributing to their accumulation in skin wounds of C57Bl/6 mice. We found that Ly6C+F4/80lo/- Mo/MΦ proliferate in the skin wounds but that Ly6C-F4/80+ MΦ do not. Additionally, Ly6C+ Mo/MΦ are found in S/G2/M phases of the cell cycle in skin wounds but not in peripheral blood, suggesting that changes in the environment of these cells may regulate their proliferation during the healing process. However, our data indicate that a variety of cytokines that have been shown to induce Mo/MΦ proliferation, either in cell culture or in other tissues, including M-CSF, IL-4, IL-6 and IL-1β, do not likely induce proliferation of Mo/MΦ in mouse skin wounds.

Materials and Methods

Animals and wound model

Male C57Bl/6 WT, IL-1R1 KO, and IL-6 KO mice (The Jackson Laboratory, Bar Harbor, ME) were housed in the animal facility of the University of Illinois at Chicago with free access to standard chow diet and water. Adult mice (age 10–12 weeks, N = 4–11/group) were subjected to excisional wounding with an 8mm biopsy punch as previously described (23). Wounds were covered with Tegaderm (3M,1626W) at all times until sacrifice to simulate clinical treatment in humans, and to provide a waterproof, sterile barrier to external contaminants.

Wounds were collected at day 1, 3, 6, and 10 post-injury along with non-injured skin samples. Prior to tissue collection, mice were anesthetized and perfused with ice cold PBS through the left ventricle of heart. After collection, tissues were either snap frozen in liquid nitrogen for protein measurements, frozen in tissue freezing medium for cryosectioning or dissociated into a single cell suspension using enzymatic digest as previously described for flow cytometry analysis (24). All animal studies were approved by the Animal care and Use Committee of the University of Illinois at Chicago.

Wound closure

Wound closure was measured in digital images taken of the wound surface. Wound closure was determined by measuring wound areas using Fiji Image J and expressing the change in area at each time point as a percentage of the original wound area ((Day 0 area – Day X area)/Day 0 area) ×100.

Histology

Cryosections (8μm thick) were cut from wounds collected on day 3, 5, 7, and 9 post-wounding. Haemotoxylin and Eosin (H&E) staining was performed in wound sections for evaluation of re-epithelialization. The percentage of re-epithelialization was calculated as [(distance traversed by epithelium from wound edges)/(distance between wound edges) ×100].

For immunofluorescence staining, sections were first blocked with PBS containing 3% BSA then incubated with primary antibodies against F4/80 and Ki67 (BD Biosciences, clone T45–2342 and Abcam, ab15580). After incubating with Rhodamine anti-rat (Jackson Immunoresearch) and Alexa Fluor 488 anti-rabbit secondary antibodies (Abcam), sections were mounted with VECTASHIELD® Antifade Mounting Media with DAPI (Vector Laboratories). Negative control sections were incubated without primary antibodies. Five distinct images were obtained with a 20×/0.5 objective from selected areas of the granulation tissue (two on each side of wounds and center of wounds. Digital images were obtained using a Nikon Instruments Eclipse 80i microscope. Staining was evaluated using Fiji ImageJ: the same threshold was used for all images, connected cells were cleaned by watershed adjustment and then DAPI+F4/80+ and DAPI+F4/80+Ki67+ positive cells were counted.

Flow cytometry

Cells from skin wounds, bone marrow, and peripheral blood were isolated from non-injured and wounded mice at day 3, 6, and 10 post-wounding. Skin wound cells were first incubated with Zombie Violet dye (Biolegend) for cell viability analysis. Then all cells were pre-incubated with anti-CD16/32 antibody (Biolegend, clone S17011E) to block the Fc receptor prior to further staining.

Cell surface antigens were labeled with anti-Ly6G-BV605 (clone 1A8), CD11b-APC/Fire750 (clone CBRM1/5), F4/80-PE (clone BM8), and Ly6C-Percp/cy5.5 (clone AL-21) antibodies (skin wound cells; Biolegend or BD Biosciences) or anti-Ly6G-BV605, CD11b-APC/Fire750, CD115-PE (clone AFS98), and Ly6C-BV421 (clone AL-21) antibodies (cells from bone marrow and peripheral blood; Biolegend or BD Biosciences). In skin, the inflammatory Mo/MΦ population was defined as Live Ly6G-CD11b+Ly6C+F4/80lo/-, while mature MΦ were gated as Live Ly6G-CD11b+ Ly6C- F4/80+. Mo were defined as Ly6G-cKit-CD11b+CD115+Ly6Chi/lo in bone marrow and Ly6G-CD11b +CD115+Ly6Chi/lo in peripheral blood.

Next, cells were fixed and permeabilized (BD Biosciences) following the manufacturer's instructions. Then, intracellular Ki67 was labeled with anti-Ki67 antibody (Abcam,

ab15580) and Alexa Fluor 488 anti-rabbit secondary antibody (Abcam, ab150077). Finally, 30 minutes prior to reading, cells were stained with FxCycle™ Far Red (ThermoFisher Scientific).

For cytokine receptor analysis, skin wound cells were first incubated with Zombie Violet dye and anti-CD16/32 antibody as described above. Then in addition to all surface myeloid cell markers, anti-CD115-PE/Dazzle594 (M-CSF receptor,clone AFS98), CD121a-PE (IL-1β receptor,clone JAMA-147), CD130-PE (surface gp130,clone 4H1B35), and CD126-APC (IL-6 receptor, clone D7715A7) antibodies (Biolegend) were added to cells in separated wells. IgG isotype control from the same clones of those antibodies were used as controls for evaluation of the surface receptors. All samples were analyzed on either LSR Fortessa with HTS (Becton Dickenson) or CytoFLEX S (Beckman Coulter) cytometers. Data were analyzed using FlowJo (FlowJo LLC).

Protein measurements

Whole wound tissues were homogenized in cold DPBS (10 μL DPBS/mg wound tissue) supplemented with 1% protease inhibitor cocktail (Sigma). Supernatants of wound homogenates were collected after centrifugation. Protein levels of M-CSF, IL-4, IL-1β, and IL-6 were determined using a custom BioLegend LEGENDplex™ kit. All samples were analyzed on CytoFLEX S (Beckman Coulter) cytometer.

Statistics

Data are expressed as mean ± SEM. Statistical significance of differences was evaluated by Mann-Whitney test or ANOVA. A value of $P<0.05$ was considered statistically significant.

Results

MΦ proliferate in skin wounds of C57Bl/6 mice

To establish the time course of healing in our wound model, wound closure was evaluated in digital images of the wound surface and re-epithelialization was assessed in H&E stained cryosections on days 3, 5, 7, and 9 post-injury. As shown in Fig 1A and 1B, wound closure and re-epithelialization progressed throughout this time period. On day 9 post-wounding, wounds still appeared open in digital images; however, H&E assessment indicated that wounds achieved complete re-epithelialization by this time point, which is consistent with previous findings that skin contraction contributes to wound closure (25). In addition, the H&E images showed that immature granulation tissue was deposited on days 5 and 7 post-injury with more mature granulation tissue evident by day 9.

To determine whether Mo/MΦ proliferate during wound healing, we first performed immunofluorescent staining of wound cryosections. The common MΦ marker F4/80 was used to identify wound MΦ while nuclear staining of Ki67 was used to indicate proliferation status. We found that MΦ (F4/80+Ki67+) proliferated in skin wounds throughout the healing process (Supplementary Fig 1A). There were abundant F4/80+ MΦ in wounds by day 3 post-injury, peaking on day 5, then declining as the wound closed (Supplementary Fig 1B). In a temporally similar pattern, MΦ (F4/80+Ki67+) were found to be proliferating on day 3,

peaked on day 5 post-injury and then declined (Supplementary Fig 1C). Thus, these data show that MΦ proliferate in mouse skin wounds.

Ly6C+ Mo/MΦ but not Ly6C- MΦ proliferate in skin wounds

To better understand the proliferation dynamics of MΦ in skin wounds, we evaluated the cell cycle in wound Mo/MΦ by flow cytometry. As shown in Fig 2A, the two dominant populations of interest were Ly6C+F4/80lo/- Mo/MΦ and Ly6C- F4/80+ MΦ. The Ly6C +/F4/80-/lo population is likely comprised mostly of infiltrating inflammatory Ly6Chi blood monocytes (7, 12). In response to injury, these cells increased both as a percentage within the total wound cell population and in absolute numbers per mg tissue weight by day 3 post-injury compared to non-injured skin. The percentage of these cells declined towards baseline during the resolution phase of healing (day 10), but cell number was maintained at a significantly higher level than non-injured skin (Fig 2B and supplementary Fig 2A).

Ki67 is present in all cell cycle phases (G1, S, G2, and M) except the resting phase (G0) (26). Therefore, by combining Ki67 labeling with the DNA dye FxCycle, we could identify cells at G0 (Ki67-FxCycle-), G1 (Ki67+FxCycle-) and S/G2/M phases (Ki67+FxCycle+). We found that injury induced increased percentages and numbers of Ly6C+F4/80lo/- Mo/MΦ that were Ki67+FxCycle+ (DNA synthesis and dividing phases of the cell cycle; S/G2/M) by day 3 post-injury; the percentage of these cells peaked on day 6 and then decreased by day 10 (Fig 2F). Numbers of Ki67+FxCycle+ Mo/MΦ (S/G2/M phases) followed a similar pattern as their percentages (Supplementary Fig 2C). These data indicate that inflammatory Ly6C+F4/80lo/- Mo/MΦ proliferate during skin wound healing.

The Ly6C-/F4/80+ population is likely comprised both of infiltrating Ly6C+/F4/80lo/- cells that have differentiated to Ly6C-/F4/80+ cells along with resident cells that are Ly6C-/F4/80+ MΦ (7, 12). Similar to Ly6C+F4/80lo/- Mo/MΦ, mature Ly6C-/F4/80+ MΦ showed a significant increase in both percentage and number after wounding compared to non-injured skin. After reaching a peak on day 3, Ly6C-/F4/80+ MΦ percentage and number declined towards baseline as the wounds closed (Fig 2D and Supplementary Fig 2B). However, unlike inflammatory Ly6C+F4/80lo/- Mo/MΦ, mature Ly6C-/F4/80+ MΦ were mainly Ki67-FxCycle- (G0 phase) and fewer were Ki67+FxCycle- (G1 phase) following injury compared to non-injured skin ($P=0.019$), with less 1% cells Ki67+FxCycle+ (S/G2/M phases) (Fig 2E, 2F and Supplementary Fig 2C). Thus, in contrast to data from models of TH2 inflammation (17), the majority of mature Ly6C-F4/80+ MΦ maintained at the resting G0 phase following skin wounding.

Mo proliferate in bone marrow but not in peripheral blood both at steady state and during wound healing

During the inflammatory phase of wound healing, bone marrow-derived cells, including Mo, infiltrate wounds from the circulation (2). Since we found proliferating Ly6C+ Mo/MΦ in wounds, we examined the cell cycle kinetics of Ly6Chi and Ly6Clo Mo in bone marrow (Ly6G-cKit-CD11b+CD115+Ly6Chi/lo) and in peripheral blood (Ly6G-CD11b +CD115+Ly6Chi/lo). Zombie dye was excluded from the staining panel due to consistently low percentages of dead cells in both bone marrow and blood samples in preliminary test

runs (<4%). Following skin wounding, numbers of Ly6Chi Mo (Ly6G-cKit-CD11b +CD115+Ly6Chi) significantly increased in bone marrow on day 6 compared to the non-injured state but Ly6Clo Mo (Ly6G-cKit-CD11b+CD115+Ly6Clo) remained at lower numbers (Fig 3B). At steady state, a proportion of both Ly6Chi and Ly6Clo Mo were Ki67+FxCycle+ (S/G2/M phases). Wounding did not change the percentage of Ki67+FxCycle+ Ly6Chi Mo (Fig 3C), but did reduce the percentage of Ki67+FxCycle+ Ly6Clo Mo and increase the percentage of Ki67-FxCycle- Ly6Clo Mo (Fig 3D), such that after injury, there were greater percentages of Ly6Chi Mo compared to Ly6Clo Mo that were Ki67+FxCycle+ on day 3 and 6 (P=0.029 and P=0.047, respectively).

In peripheral blood, Ly6Chi and Ly6Clo Mo numbers showed similar trends as in bone marrow (Fig 3F). When we analyzed the cell cycle in blood Mo populations, the majority of cells were Ki67+FxCycle- (G1 phase), with a minor fraction being Ki67-FxCycle- (G0 phase). Less than 1% of cells were Ki67+FxCycle+ (S/G2/M phases) (Fig 3G and 3H). Taken together, these data indicate that although Ly6Chi Mo proliferate in bone marrow, after they mobilize to peripheral blood, they are maintained predominantly in the G1 phase. Then, following infiltration from the blood into skin wounds, Ly6Chi Mo are again induced to enter the dividing S/G2/M phases.

IL-1 and IL-6 do not induce proliferation of Mo/MΦ in skin wounds

Although blood Ly6Chi Mo were predominantly in the G1 phase, injury increased the percentage and number of Ly6C+ Mo/MΦ at the S/G2/M phases in skin wounds. Thus, we hypothesized that changes in the microenvironment of these cells as they infiltrate wounds drives Mo/MΦ into the proliferative phases of the cell cycle. Several cytokines can promote Mo/MΦ lineage cell proliferation in different tissues (18, 20, 27–30), thus we assessed the potential roles of M-CSF, IL-4, IL-1β, and IL-6 on Mo/MΦ proliferation in skin wounds.

First, we measured M-CSF, IL-4, IL-1β, and IL-6 protein levels in non-injured skin and wound homogenate on days 1, 3, 6, and 10 after injury. Wounding lead to a rapid increase of IL-1β and IL-6 levels in skin wounds early in the healing process, which declined towards baseline levels as healing progressed (Fig 4A, 4B). Opposite to these changes, M-CSF levels tended to decline in response to injury and were maintained at a low level throughout the period assessed (Fig 4C), while IL-4 levels remained at extremely low levels near the detection level of the assay throughout the time course of healing (Fig 4D).

Next, we assessed surface expression of receptors for M-CSF (CD115), IL-4 (CD124), IL-1β (CD121a), and IL-6 (CD130 and CD126) in Ly6C+F4/80lo/- Mo/MΦ and Ly6C-F4/80+ MΦ isolated from wounds on day 6 post-injury. As shown in Fig 4E, only ~ 2% of Ly6C+F4/80lo/- Mo/MΦ expressed CD115, a percentage significantly lower than that in mature Ly6C- F4/80+ MΦ. CD124 (IL-4 receptor) and CD121a (IL-1 receptor) were expressed on both Ly6C+F4/80lo/- and Ly6C-/F4/80+ Mo/MΦ, with a lower percentage on Ly6C+F4/80lo/- Mo/MΦ compared to Ly6C-F4/80+ cells. The two receptors that can bind IL-6, CD126 (IL-6R) and CD130 (surface gp130) showed different expression patterns. CD130 was highly expressed on Ly6C+F4/80lo/- Mo/MΦ with moderate expression on Ly6C- F4/80+ MΦ. However, CD126 was rarely detected on the cell surface in either Mo/MΦ population. Finally, expression of a subset of those receptors (CD124, CD115, and

CD121a) was also evaluated on day 1 post-wounding and showed similar patterns of expression as on day 6 (Supplementary Fig 3A).

Since receptors of IL-1 and IL-6 were expressed on the cell surface of Ly6C+F4/80lo/- Mo/MΦ (CD121a: 11.2 ± 2.8% and CD130: 29.0 ± 4.5%, respectively) and protein levels of the respective cytokines were significantly elevated in response to injury, we employed IL-1R1 KO, IL-6 KO and age-matched C57Bl/6 WT control mice to study the effects of IL-1R1 and IL-6 on Mo/MΦ proliferation in skin wound healing. We assessed proliferation on day 6 post-wounding, since proliferation peaked at this time point in WT C57Bl/6 mice. As shown in Fig 4F, percentages of Ly6C+F4/80lo/- Mo/MΦ and Ly6C-F4/80+ MΦ were comparable in the wounds of IL-1R1 KO, IL-6 KO mice and their WT counterparts. Moreover, absolute numbers of Mo/MΦ were also not significantly different between genotypes (Supplementary Fig 3B). In addition, the percentages of both Ly6C+F4/80lo/- Mo/MΦ and Ly6C-F4/80+ MΦ at different cell cycle phases were also similar between the three mouse genotypes, with no significant differences between genotypes in the percentage or number of Ki67+FxCycle + Ly6C+F4/80lo/- Mo/MΦ (S/G2/M phase) (Fig 4G, 4H, and Supplementary Fig 3C).

In summary, although we found that injury leads to increases in IL-1β and IL-6 levels in wounds, and Ly6C+F4/80lo/- cells expressed receptors of IL-1 and IL-6, neither the absence of IL-1R1 nor of IL-6 influenced Mo/MΦ proliferation in wounds.

Discussion

In this study, we sought to determine whether Mo and/or MΦ proliferate in skin wounds. Our findings show for the first time that skin wounding causes inflammatory Ly6C +F4/80lo/- Mo/MΦ to enter the proliferative S/G2/M stages of the cell cycle. In addition, whereas in other tissues mature F4/80+ MΦ proliferate in response to inflammatory signals (17, 18), these cells show an opposite response to skin wounding, entering the resting G0 phase of the cell cycle. Furthermore, whereas Ly6Chi Mo are frequently found in S/G2/M phases in bone marrow, these cells are predominantly in the G1 phase in peripheral blood. Together, these data suggest that the wound environment drives the proliferation of Ly6C+ F4/80lo/- Mo/MΦ after infiltration from the blood. Finally, although levels of IL-1β and IL-6 increase in skin after wounding and Ly6C+F4/80lo/- Mo/MΦ express receptors of IL-1 and IL-6 on their cell surface, neither loss of IL-1R1 nor IL-6 affected proliferation of these cells in wounds.

In response to injury, Ly6Chi Mo are mobilized from bone marrow into peripheral blood and eventually infiltrate into wounds, where they differentiate into Ly6C+ MΦ and then Ly6C- MΦ. Prior studies suggest that this process provides the majority of MΦ involved in wound repair (1, 2, 5, 9). In agreement with previous studies (31, 32), we detected both Ly6C+ F4/80lo/- Mo/MΦ and mature Ly6C- F4/80+ MΦ accumulation in skin wounds. Whereas the numbers of Ly6C+F4/80lo/- Mo/MΦ were maintained at a relatively high level even during the later healing stages, the number of mature Ly6C-F4/80+ MΦ declined towards the non-injured skin baseline on day 10 post-wounding. Thus, the difference in the kinetics of these two Mo/MΦ populations suggests different mechanisms influencing their accumulation during the healing process. Surprisingly, we observed an Ly6C+ Mo/MΦ cell

population in non-injured skin. This population was composed of both F4/80hi/+ and F4/80lo/- cells, whereas in wounds Ly6C+ cells were almost solely F4/80lo/−. We plan on further investigating the identity of these cells in future studies.

Several studies have shown that numbers of MΦ (F4/80+ or Ly6B+) are influenced by proliferation in peritoneal cavity, lung, aorta, and adipose tissue (14–18, 20, 22). For example, pleural cavity F4/80+ MΦ proliferate in response to TH2 inflammation (17). In addition, aortic F4/80+ MΦ in atherosclerotic lesions proliferate, as indicated by a high proportion of cells in the S/G2/M phases of the cell cycle (20). Furthermore, in obese mice, a major fraction of the adipose tissue MΦ undergo cell division locally within the visceral fat pad (14, 15). In skin, Langerhans cells can proliferate while in their differentiated state under both homeostatic and inflammatory conditions (33). In agreement with these previous findings, we found proliferating MΦ (F4/80+Ki67+ cells) in skin wounds. In contrast to previous findings showing that mature MΦ proliferate, we found a significant percentage of inflammatory Ly6C+ F4/80lo/- Mo/MΦ in the DNA synthesis and dividing phases of the cell cycle (S/G2/M) in response to injury, whereas mature MΦ (Ly6C- F4/80+) showed the opposite trend, with an increased percentage of cells in the resting G0 phase. Therefore, proliferation contributes to accumulation of Ly6C+F4/80lo/- Mo/MΦ in skin wound healing, similar to a recent study using an infection model, which detected higher proliferation of Ly6C+ Mo compared to Ly6C- MΦ in mouse bladder (27). In addition to proliferation, other factors such as rates of cell infiltration, Mo differentiation, cell efflux and apoptosis may also contribute to Mo/MΦ accumulation in wounds. Future studies will be focused on the contributions of each of these processes to Mo/MΦ accumulation in wounds and the associated mechanisms.

We also assessed the influence of skin wounding on the cell cycle of Mo in bone marrow and blood, since these cells are considered to be precursors of wound Mo/MΦ (2, 9). Though about 20% of bone marrow Ly6Chi Mo were observed in S/G2/M phases both before and after skin injury, these cells were rarely in S/G2/M phases in peripheral blood. Because peripheral blood Ly6Chi Mo are likely the predominant precursors of Ly6C+ Mo/MΦ in wounds, we hypothesized that the wound environment may trigger proliferation of Ly6C+F4/80lo/- Mo/MΦ. Overall, in the tissues examined in this study, we found that cells with high Ly6C surface expression proliferate more compared to those without, as only Ly6Chi/+ Mo and/or MΦ were found in S/G2/M phases, which suggests the inflammatory Ly6C+ cells may have greater proliferating potential compared to more mature Ly6C- cells.

Next, we attempted to identify potential regulator(s) of Ly6C+F4/80lo/- Mo/MΦ proliferation in skin wounds. Previous studies have shown that several cytokines promote Mo and MΦ proliferation in inflammation (14–16, 18, 22, 27, 29, 30). Therefore, we first investigated protein levels of those cytokines in wounds, including M-CSF, IL-4, IL-1β, and IL-6. First, M-CSF, which has been reported to be a key regulator of resident MΦ proliferation during inflammation (18, 22), showed a reduction in protein levels post-wounding and its receptor (CD115) was expressed only at low levels on Ly6C+F4/80lo/- Mo/MΦ in wounds. Next, IL-4 protein levels were extremely low in skin wounds throughout the healing process, close to the detection limit of the assay. This is consistent with our previous data (24) and that of others (34), showing undetectable levels of IL-4 or IL-13 in

skin wounds. Therefore, it is not likely that either IL-4 or M-CSF promotes proliferation of Ly6C+F4/80lo/- Mo/MΦ in our model of skin wound healing.

In contrast, levels of pro-inflammatory cytokines IL-1β and IL-6 rapidly increased following skin wounding and cell surface receptors involved in their signaling pathways (CD121a and CD130, respectively) were expressed on Ly6C+F4/80lo/- Mo/MΦ. Thus, we hypothesized that IL-1 and/or IL-6 signaling might mediate Ly6C+F4/80lo/- Mo/MΦ proliferation. However, neither IL-1R1 nor IL-6 KO mice showed significant differences in Ly6C +F4/80lo/- Mo/MΦ proliferation compared to their WT counterparts. Thus, when comparing to reports in the literature, our data indicate that the pathways involved in regulating Mo/MΦ proliferation are likely context-specific. Previous studies reported that osteopontin and MCP-1 play a key role in regulating adipose tissue MΦ proliferation (14, 28). Moreover, cell intrinsic pathways such as lysosomal lipolysis may affect bone-marrow derived MΦ activation and proliferation in response to infection *in vitro* (35, 36). Hence, we are planning future studies to determine the influence of these and other potential factors on Mo/MΦ proliferation during skin wound healing.

One limitation of our study is the use of KO mouse models as the life-long loss of either IL-1R1 or IL-6 may cause systemic changes which could affect inflammatory and healing responses and confound interpretation of our data. However, we and others have shown that the inflammatory response and wound healing of IL-1R KO mice are only subtly altered compared to WT controls (13, 37). Additionally, though previous studies have reported that IL-6 KO mice exhibit delayed healing (38, 39), we did not observe any significant difference in the Mo/MΦ response or in wound closure between IL-6 KO mice and their WT counterparts in our study. The differing results between previous studies and ours may be due to different injury models, wound sizes and mouse strains.

Our findings may have implications for chronic inflammation associated with impaired healing in diabetes and other wound healing disorders. Impaired wound healing is often associated with persistent accumulation of Mo/MΦ, although the mechanisms involved remain to be elucidated (1, 3, 23). Our data highlight the possibility that proliferation of Ly6C+F4/80lo/- Mo/MΦ contribute to their enhanced and persistent accumulation in chronic/non-healing wounds, contributing to impaired healing (4, 23). Future studies should focus on the potential role of Mo/MΦ proliferation in the establishment of chronic inflammation in wounds.

In summary, we demonstrate that inflammatory Ly6C+F4/80lo/- Mo proliferate, and that mature Ly6C-F4/80+ MΦ do not proliferate, in response to skin injury and that such proliferation may contribute to Mo/MΦ accumulation following injury. This injury-induced Mo/MΦ proliferation is likely regulated by the wound environment; however, cytokines previously reported to induce Mo/MΦ proliferation, including M-CSF, IL-4, IL-1β, and IL-6 do not appear to promote wound Mo/MΦ proliferation.

Supplementary Material

Refer to Web version on PubMed Central for supplementary material.

Acknowledgments

All authors thank Dr. Luisa A. DiPietro and Dr. Giamila Fantuzzi for their input on aspects of presentation of this manuscript.

Funding

This work was supported by a grant from the National Institutes of Health R01GM092850 to T.J.K.

Abbreviations

IL-1β	interleukin-1 beta
IL-1R1	interleukin-1 receptor 1
IL-4	interleukin-4
IL-6	interleukin-6
KO	knockout
M-CSF	macrophage colony-stimulating factor
Mo/MΦ	monocyte/macrophages

References

1. Eming SA, Martin P, and Tomic-Canic M 2014 Wound repair and regeneration: mechanisms, signaling, and translation. Science translational medicine 6: 265sr266.
2. Koh TJ, and DiPietro LA 2011 Inflammation and wound healing: the role of the macrophage. Expert Rev Mol Med 13: e23. [PubMed: 21740602]
3. Mirza R, DiPietro LA, and Koh TJ 2009 Selective and specific macrophage ablation is detrimental to wound healing in mice. The American journal of pathology 175: 2454–2462. [PubMed: 19850888]
4. Novak ML, and Koh TJ 2013 Macrophage phenotypes during tissue repair. Journal of leukocyte biology 93: 875–881. [PubMed: 23505314]
5. Gurtner GC, Werner S, Barrandon Y, and Longaker MT 2008 Wound repair and regeneration. Nature 453: 314–321. [PubMed: 18480812]
6. Yanez DA, Lacher RK, Vidyarthi A, and Colegio OR 2017 The role of macrophages in skin homeostasis. Pflugers Archiv : European journal of physiology 469: 455–463. [PubMed: 28233123]
7. Krzyszczyk P, Schloss R, Palmer A, and Berthiaume F 2018 The Role of Macrophages in Acute and Chronic Wound Healing and Interventions to Promote Pro-wound Healing Phenotypes. Frontiers in physiology 9: 419. [PubMed: 29765329]
8. Boniakowski AE, Kimball AS, Jacobs BN, Kunkel SL, and Gallagher KA 2017 Macrophage-Mediated Inflammation in Normal and Diabetic Wound Healing. Journal of immunology 199: 17–24.
9. Swirski FK, Hilgendorf I, and Robbins CS 2014 From proliferation to proliferation: monocyte lineage comes full circle. Seminars in immunopathology 36: 137–148. [PubMed: 24435095]
10. Yona S, Kim KW, Wolf Y, Mildner A, Varol D, Breker M, Strauss-Ayali D, Viukov S, Guilliams M, Misharin A, Hume DA, Perlman H, Malissen B, Zelzer E, and Jung S 2013 Fate mapping reveals origins and dynamics of monocytes and tissue macrophages under homeostasis. Immunity 38: 79–91. [PubMed: 23273845]
11. Varol C, Landsman L, Fogg DK, Greenshtein L, Gildor B, Margalit R, Kalchenko V, Geissmann F, and Jung S 2007 Monocytes give rise to mucosal, but not splenic, conventional dendritic cells. The Journal of experimental medicine 204: 171–180. [PubMed: 17190836]

12. Italiani P, and Boraschi D 2014 From Monocytes to M1/M2 Macrophages: Phenotypical vs. Functional Differentiation. Frontiers in immunology 5: 514. [PubMed: 25368618]

13. Barman PK, Pang J, Urao N, and Koh TJ 2019 Skin Wounding-Induced Monocyte Expansion in Mice Is Not Abrogated by IL-1 Receptor 1 Deficiency. Journal of immunology 202: 2720–2727.

14. Amano SU, Cohen JL, Vangala P, Tencerova M, Nicoloro SM, Yawe JC, Shen Y, Czech MP, and Aouadi M 2014 Local proliferation of macrophages contributes to obesity-associated adipose tissue inflammation. Cell metabolism 19: 162–171. [PubMed: 24374218]

15. Hashimoto D, Chow A, Noizat C, Teo P, Beasley MB, Leboeuf M, Becker CD, See P, Price J, Lucas D, Greter M, Mortha A, Boyer SW, Forsberg EC, Tanaka M, van Rooijen N, Garcia-Sastre A, Stanley ER, Ginhoux F, Frenette PS, and Merad M 2013 Tissue-resident macrophages self-maintain locally throughout adult life with minimal contribution from circulating monocytes. Immunity 38: 792–804. [PubMed: 23601688]

16. Isbel NM, Nikolic-Paterson DJ, Hill PA, Dowling J, and Atkins RC 2001 Local macrophage proliferation correlates with increased renal M-CSF expression in human glomerulonephritis. Nephrology, dialysis, transplantation : official publication of the European Dialysis and Transplant Association - European Renal Association 16: 1638–1647.

17. Jenkins SJ, Ruckerl D, Cook PC, Jones LH, Finkelman FD, van Rooijen N, MacDonald AS, and Allen JE 2011 Local macrophage proliferation, rather than recruitment from the blood, is a signature of TH2 inflammation. Science 332: 1284–1288. [PubMed: 21566158]

18. Jenkins SJ, Ruckerl D, Thomas GD, Hewitson JP, Duncan S, Brombacher F, Maizels RM, Hume DA, and Allen JE 2013 IL-4 directly signals tissue-resident macrophages to proliferate beyond homeostatic levels controlled by CSF-1. The Journal of experimental medicine 210: 2477–2491. [PubMed: 24101381]

19. Minutti CM, Knipper JA, Allen JE, and Zaiss DM 2017 Tissue-specific contribution of macrophages to wound healing. Seminars in cell & developmental biology 61: 3–11. [PubMed: 27521521]

20. Robbins CS, Hilgendorf I, Weber GF, Theurl I, Iwamoto Y, Figueiredo JL, Gorbatov R, Sukhova GK, Gerhardt LM, Smyth D, Zavitz CC, Shikatani EA, Parsons M, van Rooijen N, Lin HY, Husain M, Libby P, Nahrendorf M, Weissleder R, and Swirski FK 2013 Local proliferation dominates lesional macrophage accumulation in atherosclerosis. Nature medicine 19: 1166–1172.

21. Perry VH, and Teeling J 2013 Microglia and macrophages of the central nervous system: the contribution of microglia priming and systemic inflammation to chronic neurodegeneration. Seminars in immunopathology 35: 601–612. [PubMed: 23732506]

22. Le Meur Y, Tesch GH, Hill PA, Mu W, Foti R, Nikolic-Paterson DJ, and Atkins RC 2002 Macrophage accumulation at a site of renal inflammation is dependent on the M-CSF/c-fms pathway. Journal of leukocyte biology 72: 530–537. [PubMed: 12223521]

23. Mirza RE, Fang MM, Weinheimer-Haus EM, Ennis WJ, and Koh TJ 2014 Sustained inflammasome activity in macrophages impairs wound healing in type 2 diabetic humans and mice. Diabetes 63: 1103–1114. [PubMed: 24194505]

24. Mirza RE, Fang MM, Ennis WJ, and Koh TJ 2013 Blocking interleukin-1beta induces a healing-associated wound macrophage phenotype and improves healing in type 2 diabetes. Diabetes 62: 2579–2587. [PubMed: 23493576]

25. Chen L, Mirza R, Kwon Y, DiPietro LA, and Koh TJ 2015 The murine excisional wound model: Contraction revisited. Wound repair and regeneration : official publication of the Wound Healing Society [and] the European Tissue Repair Society 23: 874–877.

26. Vignon C, Debeissat C, Georget MT, Bouscary D, Gyan E, Rosset P, and Herault O 2013 Flow cytometric quantification of all phases of the cell cycle and apoptosis in a two-color fluorescence plot. PloS one 8: e68425. [PubMed: 23935867]

27. Dixit A, Bottek J, Beerlage AL, Schuettpelz J, Thiebes S, Brenzel A, Garbers C, Rose-John S, Mittrucker HW, Squire A, and Engel DR 2018 Frontline Science: Proliferation of Ly6C(+) monocytes during urinary tract infections is regulated by IL-6 trans-signaling. Journal of leukocyte biology 103: 13–22. [PubMed: 28882904]

28. Tardelli M, Zeyda K, Moreno-Viedma V, Wanko B, Grun NG, Staffler G, Zeyda M, and Stulnig TM 2016 Osteopontin is a key player for local adipose tissue macrophage proliferation in obesity. Molecular metabolism 5: 1131–1137. [PubMed: 27818939]
29. Vela JM, Molina-Holgado E, Arevalo-Martin A, Almazan G, and Guaza C 2002 Interleukin-1 regulates proliferation and differentiation of oligodendrocyte progenitor cells. Molecular and cellular neurosciences 20: 489–502. [PubMed: 12139924]
30. Vesey DA, Cheung C, Cuttle L, Endre Z, Gobe G, and Johnson DW 2002 Interleukin-1beta stimulates human renal fibroblast proliferation and matrix protein production by means of a transforming growth factor-beta-dependent mechanism. The Journal of laboratory and clinical medicine 140: 342–350. [PubMed: 12434136]
31. Olingy CE, San Emeterio CL, Ogle ME, Krieger JR, Bruce AC, Pfau DD, Jordan BT, Peirce SM, and Botchwey EA 2017 Non-classical monocytes are biased progenitors of wound healing macrophages during soft tissue injury. Scientific reports 7: 447. [PubMed: 28348370]
32. Willenborg S, Lucas T, van Loo G, Knipper JA, Krieg T, Haase I, Brachvogel B, Hammerschmidt M, Nagy A, Ferrara N, Pasparakis M, and Eming SA 2012 CCR2 recruits an inflammatory macrophage subpopulation critical for angiogenesis in tissue repair. Blood 120: 613–625. [PubMed: 22577176]
33. Deckers J, Hammad H, and Hoste E 2018 Langerhans Cells: Sensing the Environment in Health and Disease. Frontiers in immunology 9: 93. [PubMed: 29449841]
34. Daley JM, Brancato SK, Thomay AA, Reichner JS, and Albina JE 2010 The phenotype of murine wound macrophages. Journal of leukocyte biology 87: 59–67. [PubMed: 20052800]
35. Huang SC, Everts B, Ivanova Y, O'Sullivan D, Nascimento M, Smith AM, Beatty W, Love-Gregory L, Lam WY, O'Neill CM, Yan C, Du H, Abumrad NA, Urban JF Jr., Artyomov MN, Pearce EL, and Pearce EJ 2014 Cell-intrinsic lysosomal lipolysis is essential for alternative activation of macrophages. Nature immunology 15: 846–855. [PubMed: 25086775]
36. Ruckerl D, and Allen JE 2014 Macrophage proliferation, provenance, and plasticity in macroparasite infection. Immunological reviews 262: 113–133. [PubMed: 25319331]
37. Thomay AA, Daley JM, Sabo E, Worth PJ, Shelton LJ, Harty MW, Reichner JS, and Albina JE 2009 Disruption of interleukin-1 signaling improves the quality of wound healing. The American journal of pathology 174: 2129–2136. [PubMed: 19389930]
38. Gallucci RM, Sugawara T, Yucesoy B, Berryann K, Simeonova PP, Matheson JM, and Luster MI 2001 Interleukin-6 treatment augments cutaneous wound healing in immunosuppressed mice. Journal of interferon & cytokine research : the official journal of the International Society for Interferon and Cytokine Research 21: 603–609.
39. Lin ZQ, Kondo T, Ishida Y, Takayasu T, and Mukaida N 2003 Essential involvement of IL-6 in the skin wound-healing process as evidenced by delayed wound healing in IL-6-deficient mice. Journal of leukocyte biology 73: 713–721. [PubMed: 12773503]

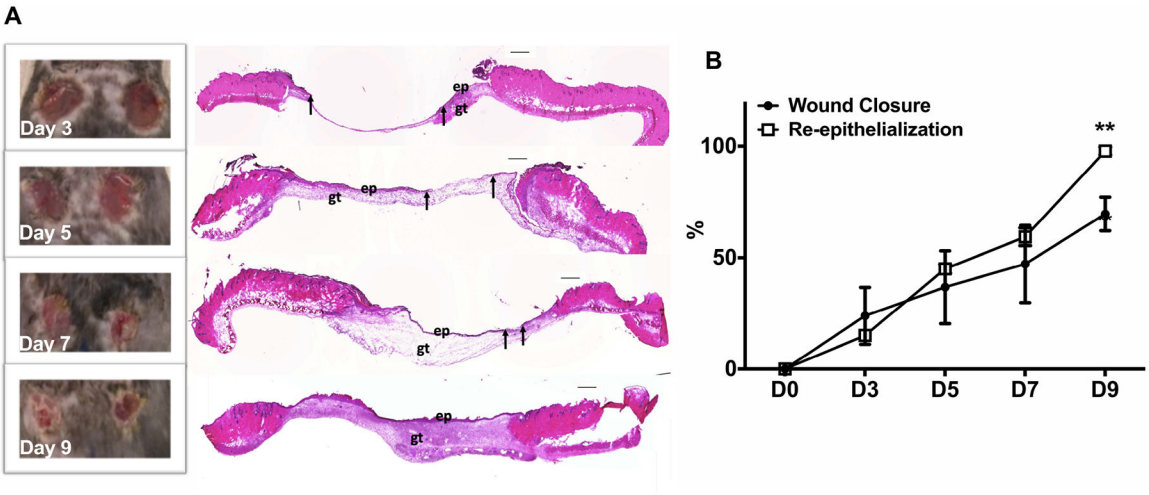

Figure 1. Model of skin wound healing in C57Bl/6 mice.

(**A**) Representative images of wound closure by digital pictures (left) and H&E stained cryosections (right) on day 3, 5, 7, and 9 post-injury. ep, epithelium; gt, granulation tissue. Arrows indicate ends of epithelial tongues, scale bar = 0.5mm. (**B**) Wound closure was calculated as 100% minus percentage of open area to the initial wound size on day 0. Re-epithelization was evaluated as percentage of epithelial tongues to the initial wound length in H&E stained cryosections. Data expressed as mean ± SEM for 4 mice per group and are representative of healing in all subsequent experiments of study; *****P < 0.05 *vs* wound closure by digital pictures by ANOVA.

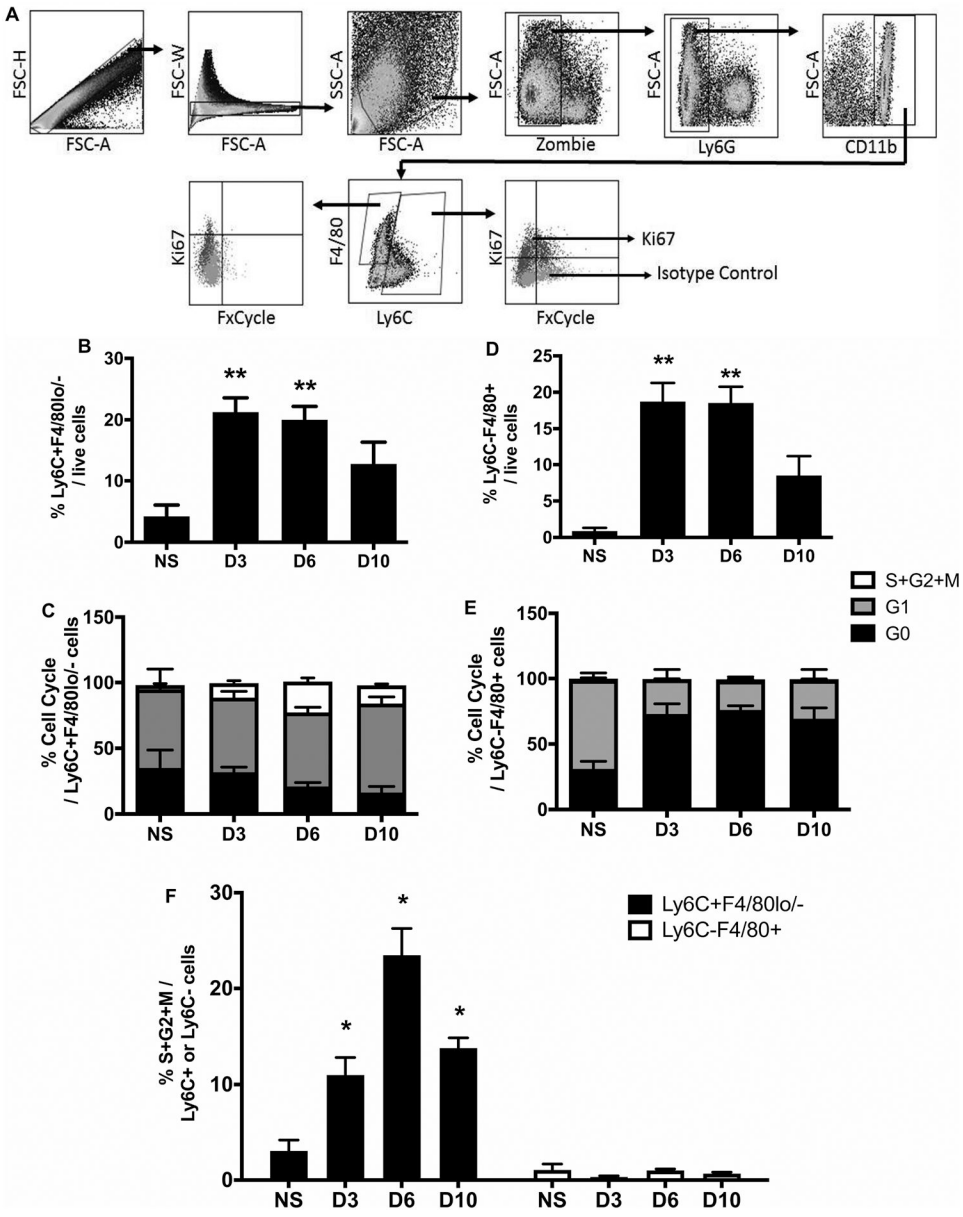

Figure 2. Skin wounding increases proliferation of Ly6C+ Mo/MΦ but not mature Ly6C- MΦ.

(**A**) Representative flow cytometric images showing proliferative profiles of Ly6C+F4/80lo/- Mo/MΦ and Ly6C-F4/80+ MΦ in skin wounds on day 6 post-injury. (**B**) and (**D**) Percentages of Ly6C+F4/80lo/- Mo/MΦ and Ly6C-F4/80+ MΦ of total live cells in normal skin (n=4) and wounds on days 3 (n=6), 6 (n=9), and 10 (n=7) post-injury. (**C**) and (**E**) Percentages of Ki67-FxCycle- cells (G0 phase, black), Ki67+FxCycle- cells (G1 phase, grey), and Ki67+FxCycle+ cells (S/G2/M phases, empty) in Ly6C+F4/80lo/- Mo/MΦ and Ly6C-F4/80+ MΦ. (**F**) Comparison of Ki67+FxCycle+ cells (S/G2/M phases) in Ly6C +F4/80lo/- Mo/MΦ (black bars) and Ly6C-F4/80+ MΦ (open bars) during wound healing. For each graph, data were pooled over three separate time course experiments; sample sizes given are pooled over experiments. Data expressed as mean ± SEM; ***P* < 0.05 or ****P* < 0.01 *vs* non-injured skin group by ANOVA.

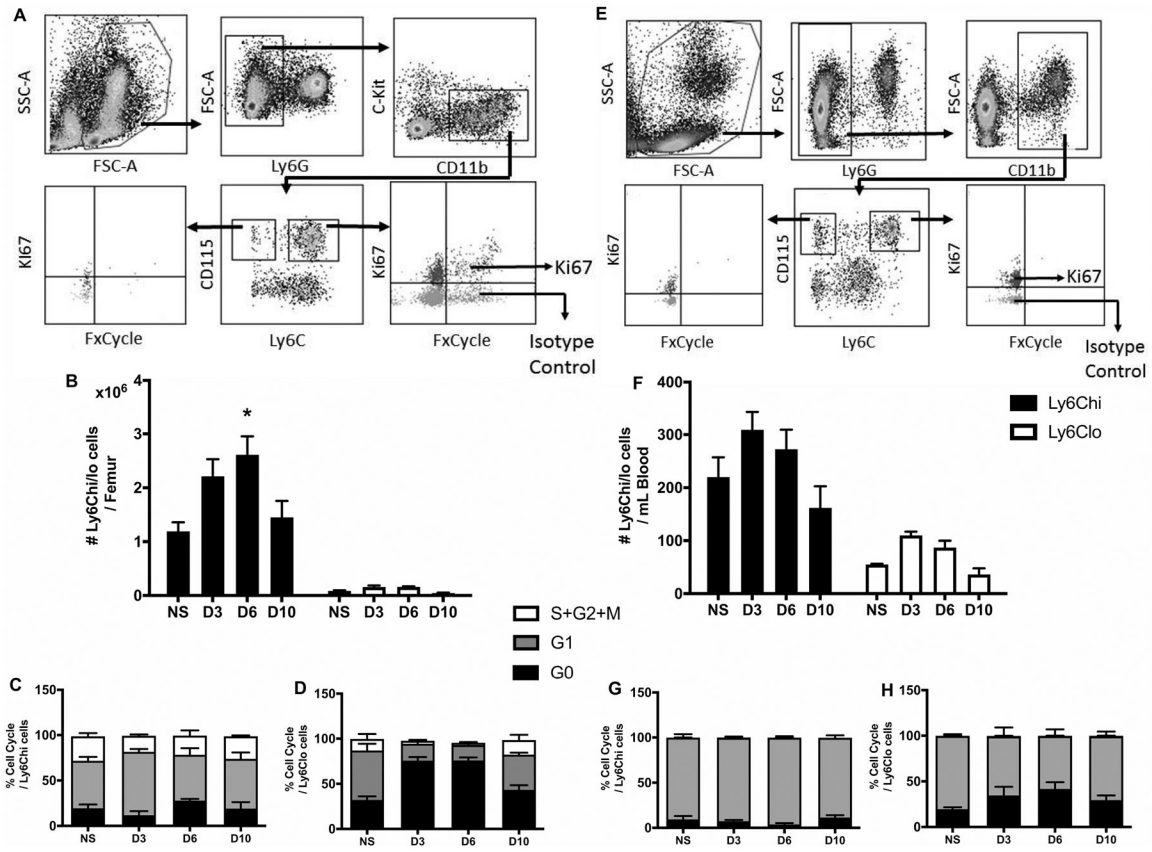

Figure 3. Mo proliferate in bone marrow but not in peripheral blood during wound healing.

(**A**) and (**E**) Representative flow cytometric images showing proliferative profiles of Ly6Chi Mo and Ly6Clo MΦ in bone marrow (left) and peripheral blood (right). (**B**) and (**F**) Comparison of Ly6Chi *vs* Ly6Clo Mo in bone marrow (Representative flow cytometric images showing proliferative profiles of Ly6Chi Mo and Ly6Clo MΦ in bone marrow (left) and peripheral blood (right) during wound healing. (**C**), (**D**), (**G**) and (**H**) Percentage of Ly6Chi and Ly6Clo Mo in different phases of cell cycle in bone marrow (left) and peripheral blood (right). For each graph, data were pooled over two separate time course experiments; sample sizes given are pooled over experiments. Data expressed as mean ± SEM for 4 mice per group; *****P < 0.05 or ******P < 0.01 *vs* non-injured group by ANOVA.

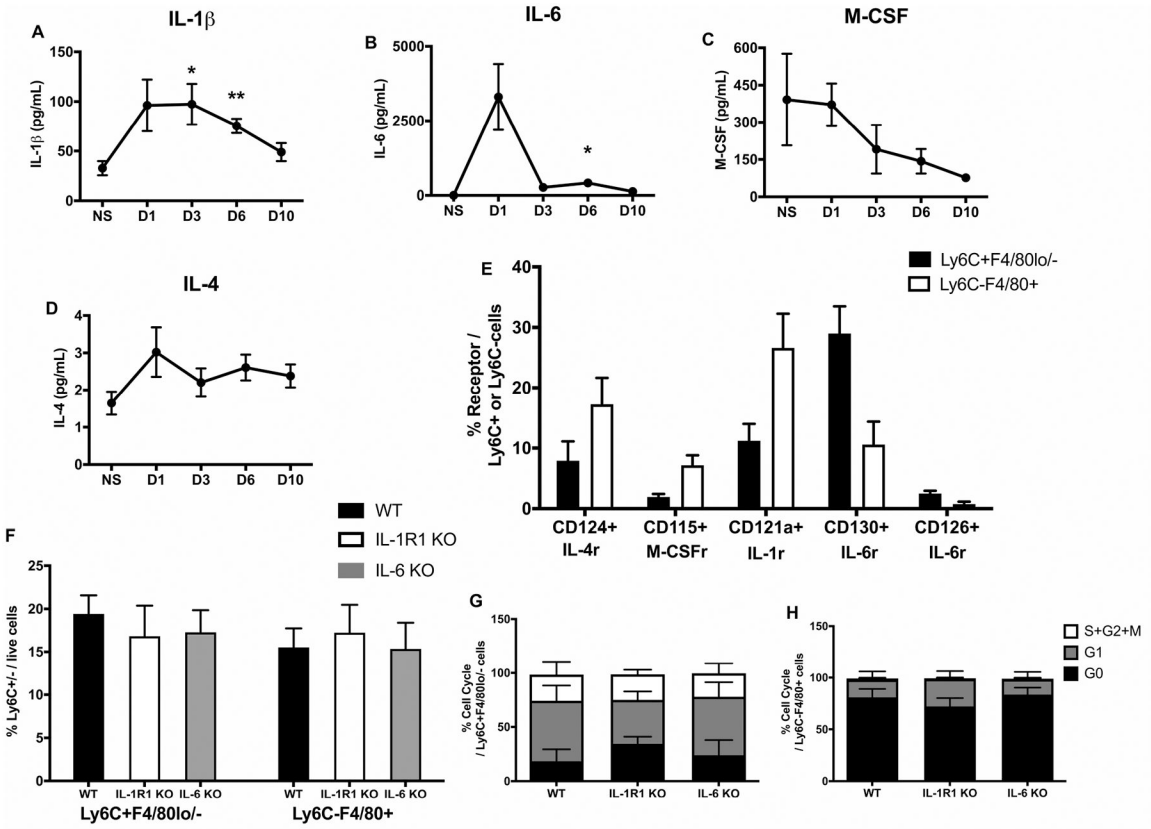

Figure 4. Injury-induced alteration of IL-1β and IL-6 levels does not induce proliferation of Mo/MΦ in skin wounds.

(**A**) to (**D**) Protein levels of IL-1β, IL-6, M-CSF, and IL-4 were measured in tissue homogenates of non-injured skin and wounds on day 1 (n=3), 3 (n=4), 6 (n=4), and 10 (n=4) by a custom multiplex kit via flow cytometry. (**E**) Surface expression of CD124 (IL-4 receptor), CD115 (M-CSF receptor), CD121a (IL-1 receptor), CD130, and CD126 (IL-6 receptors) evaluated by flow cytometry in Ly6C+F4/80lo/- Mo/MΦ (black bars) and Ly6C-F4/80+ MΦ (open bars) in skin wounds on day 6 post-injury (n=4). (**F**) Percentages of either Ly6C+F4/80lo/- Mo/MΦ or Ly6C-F4/80+ MΦ in WT (black bar, n=11), IL-1R1 KO (open bar, n=4), and IL-6 KO (grey bar, n=8) in skin wounds on day 6 post-wounding. (**G**) and (**H**) Cell cycle profiles of Ly6C+F4/80lo/- Mo/MΦ or Ly6C-F4/80+ MΦ in WT, IL-1R1 KO, and IL-6 KO mice. For each graph, data were pooled over two separate experiments; sample sizes given are pooled over experiments. Data expressed as mean ± SEM; ***P* < 0.05 or ****P* < 0.01 *vs* non-injured group by ANOVA.